Electronic Supplementary Material (ESI) for Soft Matter.

Supplementary Information

An organic/inorganic hybrid soft material for supramolecular adhesion

Yunfei Zhang, Wenchang Yi, Jia Pan, Song Liu*, & Shengyi Dong*

Y. Zhang, W. Yi, J. Pan, Prof. S. Liu and Prof. S. Dong

College of Chemistry and Chemical Engineering, Hunan University, Changsha 410082, China

*To whom correspondence should be addressed.

E-mail: dongsy@hnu.edu.cn; liusong@hnu.edu.cn

Contents

1. Materials and methods

DL-thioctic acid (**TA**) was purchased from Shanghai Aladdin Biochemical Technology Co., Ltd (Shanghai, China). **MoS_2** was purchased from Innochem. Other solvents and materials were commercially obtained and used directly. NMR spectra were collected on a Bruker 400 MHz with TMS as the internal standard. Infrared (IR) spectra were collected on a Thermo Scientific Nicolet iS10 FT-IR spectrometer. Thermogravimetric analysis (TGA) was carried out using a TG 5500, and the heating rate was 20 °C min^{-1} from 30 to 600 °C in nitrogen atmosphere. X-ray photoelectron spectroscopy (XPS) was obtained by Thermo ESCALAB 250XI. Differential scanning calorimeter (DSC) measurements were obtained by a TAQ200 with a heating rate of 10 °C from -80 to 100 °C in nitrogen atmosphere. Scanning electron microscopy (SEM) images were collected on Sigma 300. Atomic force microscope (AFM) images were collected on Bruker. Rheology measurements were performed on an Anton Paar MCR 92. The laminator model PP15 was chosen with 15 mm of diameter and 1 mm of gap. Stress-strain curves were tested by universal testing machine (Posi Test AT-A). Dynamic thermomechanical analysis (DMA) was performed on a DMA 8000-PerkinElmer using shear model.

2. Preparation of poly[TA-MoS_2]

A mixture of **TA** (10.00 g) and **MoS_2** (0.99 g) was heated and stirred in a sample bottle at 130 °C for 2 hours. Weight ratio was used in this study.

3. 3D FDM printing

The filament printing method was conducted using a short-range extrusion 3D printer (WiibooxSweetib, China). The printing temperature of the extruder was 94–96 °C, and the printing speed was 7 mm s^{-1}. The models were developed using the CAD software (AutoCAD, Autodesk), and slicing was performed using the Crua slicer software.

4. Statistical analysis

The SPSS software (version 27) was performed for the statistical analysis. Duncan's new multiple range test method was used to statistically analyze the extraction process. The P less than 0.05 was considered statistically significant. The different letters on the figures indicate the mean value are statistically different at the P less than 0.05 level.

5. The preparation and characterization of poly[TA-MoS_2]

Table S1. Contact angle and density of poly[**TA-MoS_2**]

Poly[**TA-MoS_2**]	1: 1	5: 1	10: 1	100: 1
Contact angle	72.45°	70.85°	64.20°	79.42°
Density (g/cm^3)	1.77	1.27	1.17	1.13

6. X-ray photoelectron spectroscopy of poly[TA-MoS_2]

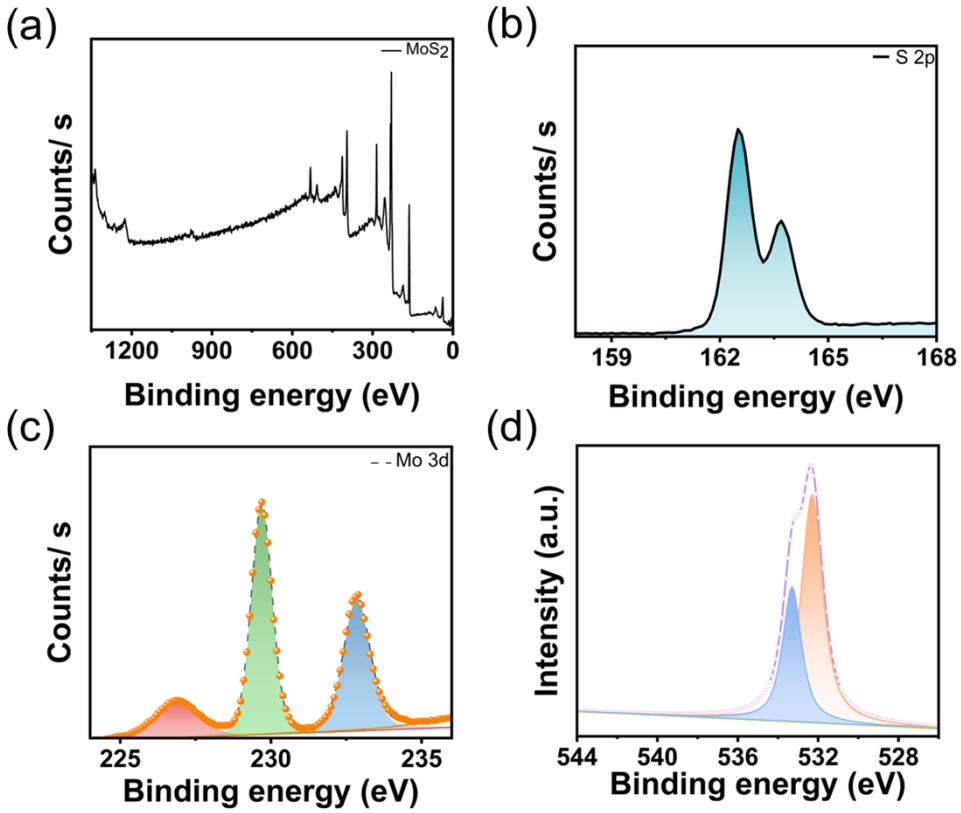

Figure S1. XPS spectra: (a) **MoS_2** survey spectrum; (b) Mo 3d of **MoS_2**; (c) S 2p of **MoS_2**; (d) O 1s of **TA**.

7. Scanning electron microscopy (SEM) of poly[TA-MoS_2]

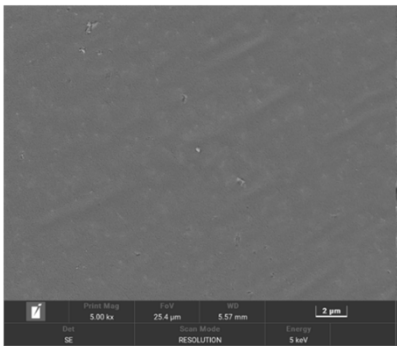

Figure S2. SEM image of poly[**TA-MoS_2**] (**TA**: **MoS_2** = 1: 1).

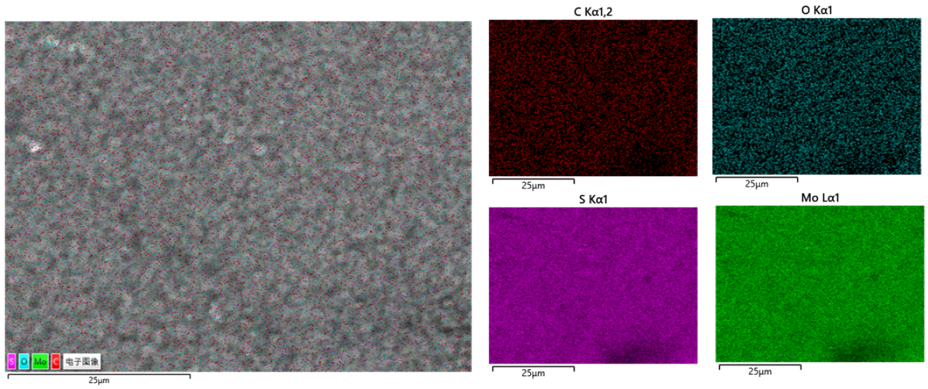

Figure S3. EDS (mapping) images of poly[**TA-MoS_2**] (**TA**: **MoS_2** = 1: 1).

8. Atomic force microscope (AFM) of poly[TA-MoS_2]

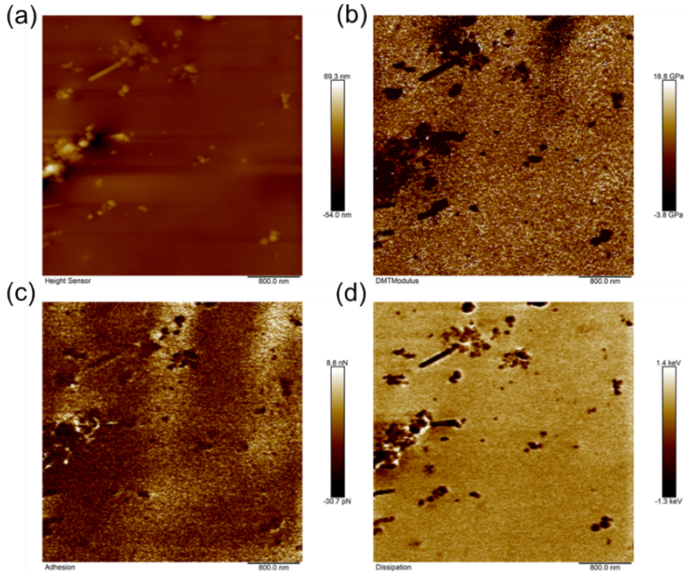

Figure S4. AFM of poly[**TA-MoS_2**]: (a) height, (b) DMT modulus, (c) adhesion, (d) dissipation (**TA**: **MoS_2** = 1: 1).

9. Thermogravimetric analysis (TGA) of poly[TA-MoS_2]

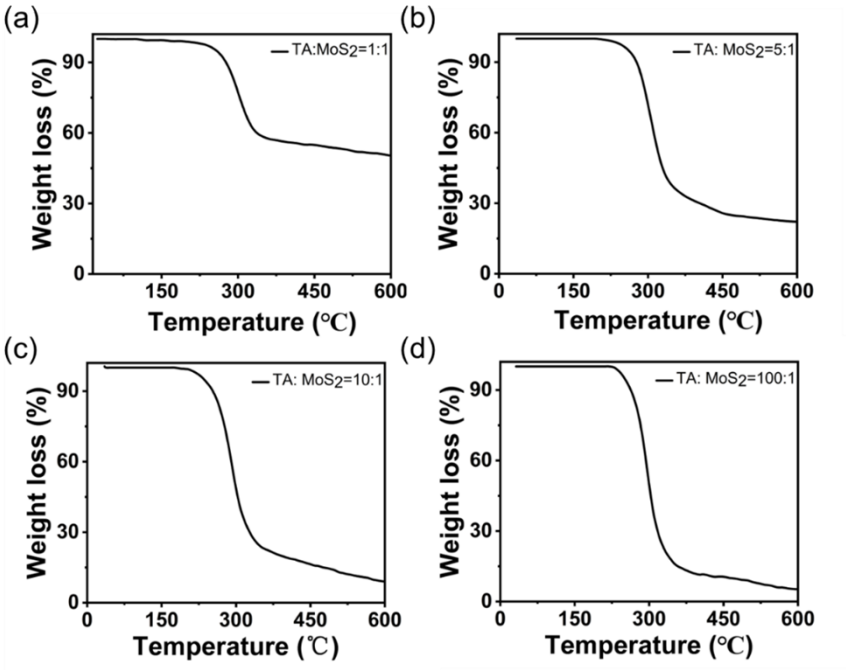

Figure S5. TG spectra of poly[**TA-MoS_2**]: (a) **TA**: **MoS_2** = 1: 1; (b) **TA**: **MoS_2** = 5: 1; (c) **TA**: **MoS_2** = 10: 1; (d) **TA**: **MoS_2** = 100: 1.

10. ^{1}H NMR spectra of poly[TA-MoS_2]

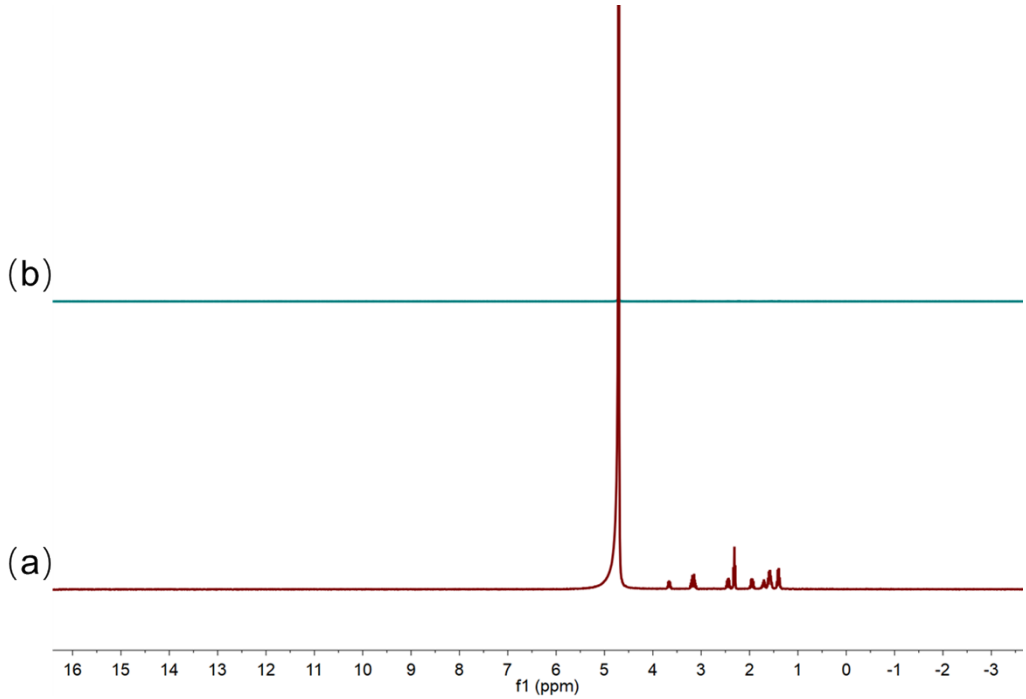

Figure S6. ^{1}H NMR spectra (400 MHz, D_2O, room temperature): (a) **TA**; (b) poly[**TA-MoS_2**]-35 day **(TA**: **MoS_2** = 1: 1).

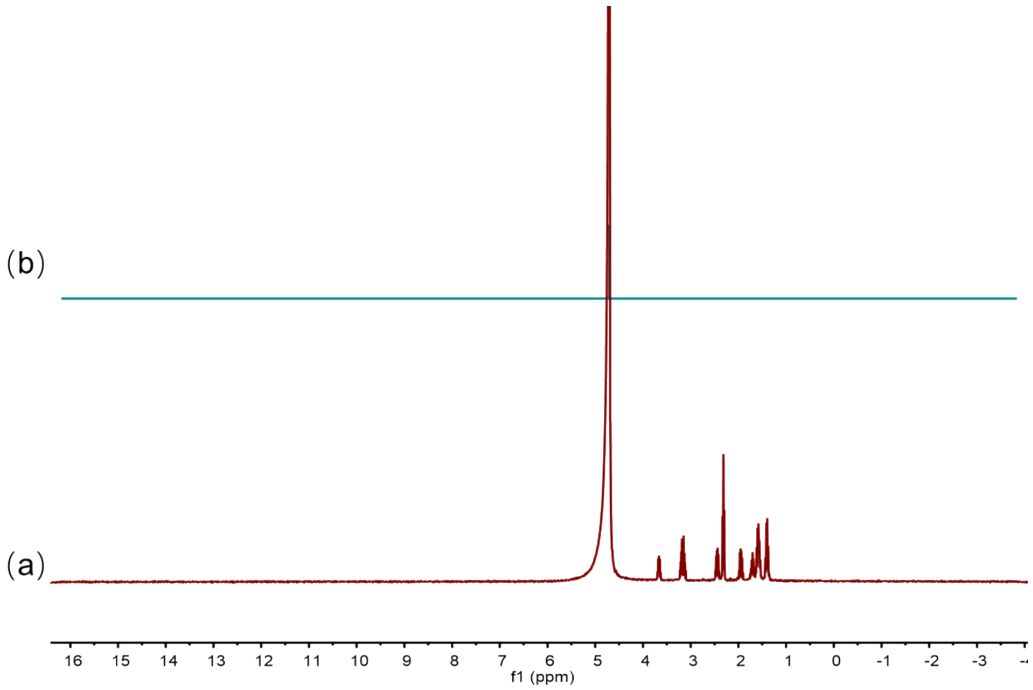

Figure S7. ^{1}H NMR spectra (400 MHz, D_2O, room temperature): (a) **TA**; (b) poly[**TA**-$\mathbf{MoS_2}$]-35 day (**TA**: $\mathbf{MoS_2}$ = 5: 1).

11. FT-IR spectra of poly[TA-MoS_2]

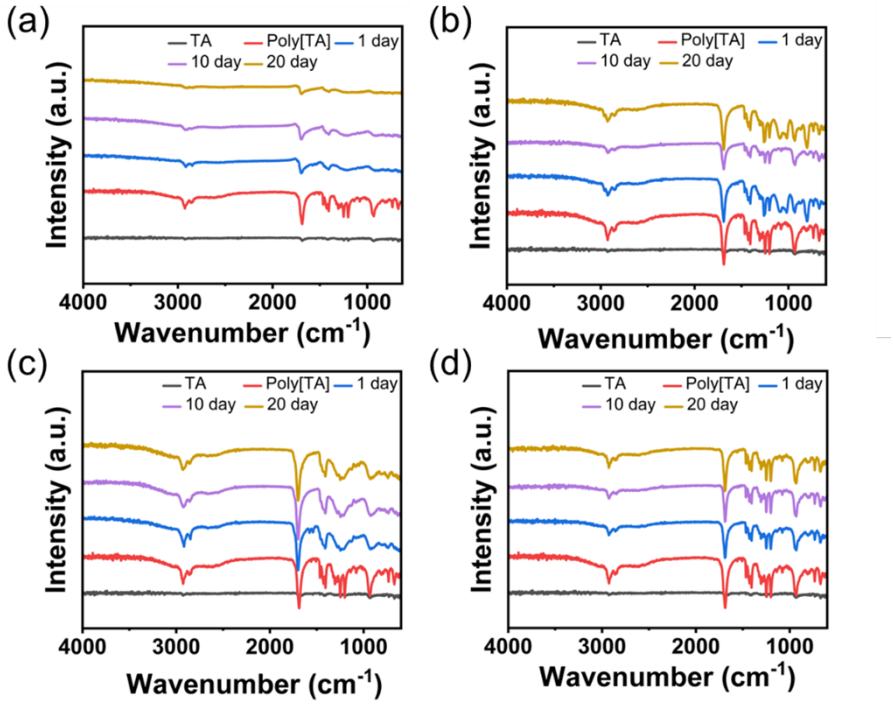

Figure S8. FT-IR spectra of poly[**TA**-$\mathbf{MoS_2}$]: (a) **TA**: $\mathbf{MoS_2}$ = 1: 1; (b) **TA**: $\mathbf{MoS_2}$ = 5: 1; (c) **TA**: $\mathbf{MoS_2}$ = 10: 1; (d) **TA**: $\mathbf{MoS_2}$ = 100: 1.

12. Differential scanning calorimeter (DSC) measurements of poly[TA-MoS_2]

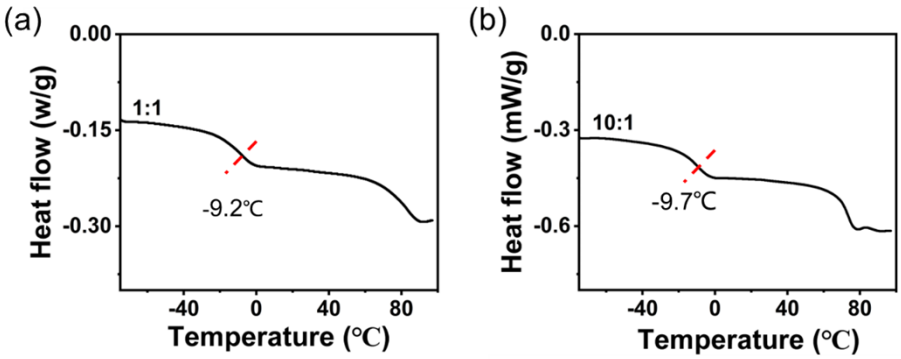

Figure S9. DSC spectra of poly[**TA-MoS_2**]: (a) **TA**: **MoS_2** = 1:1; (b) **TA**: **MoS_2** = 10:1.

13. Dynamic thermodynamic Analysis (DMA) tests of poly[TA-MoS_2]

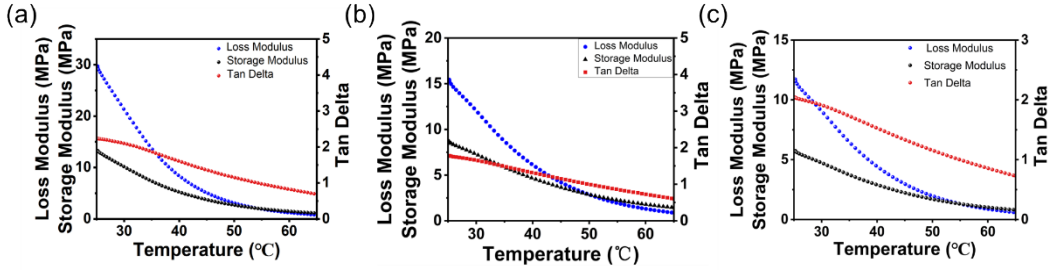

Figure S10. DMA tests of poly[**TA-MoS_2**]: (a) **TA**: **MoS_2** = 5: 1; (b) **TA**: **MoS_2** = 10: 1; (c) **TA**: **MoS_2** = 100: 1.

14. Elasticity and fatigue resistance

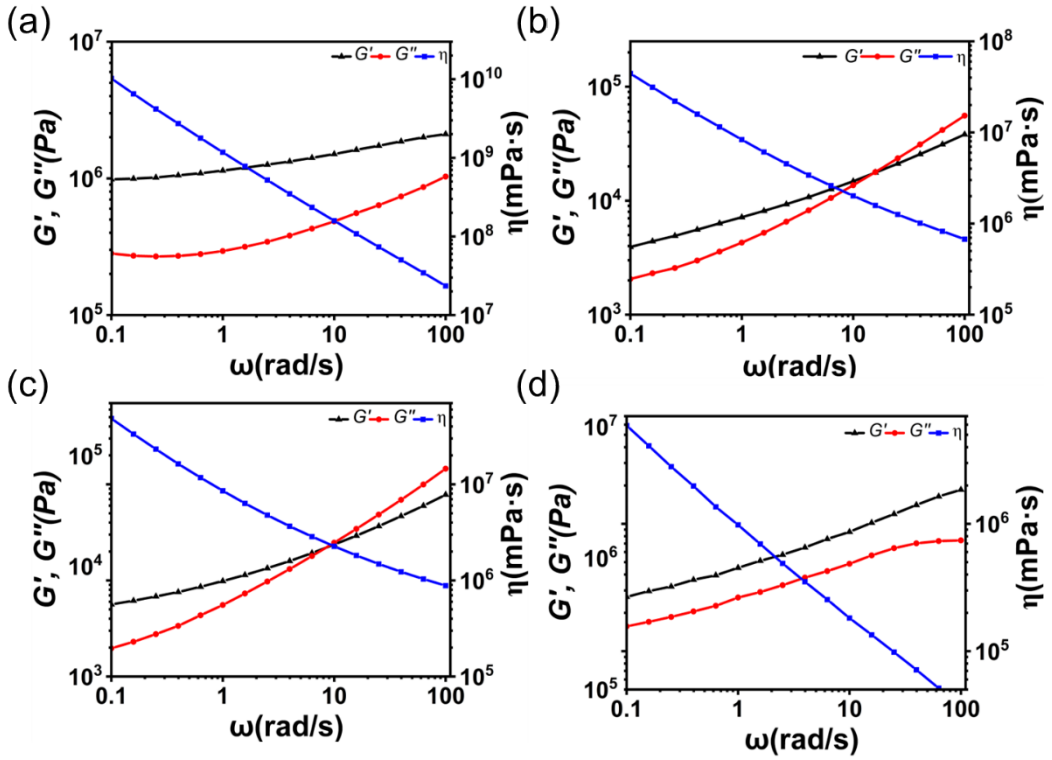

Figure 11. Storage (*G'*), loss (*G''*) moduli and viscosity (η) of poly[**TA-MoS$_2$**] at room temperature. (a) 1: 1; (b) 5: 1; (c) 10: 1; and (d) 100: 1.

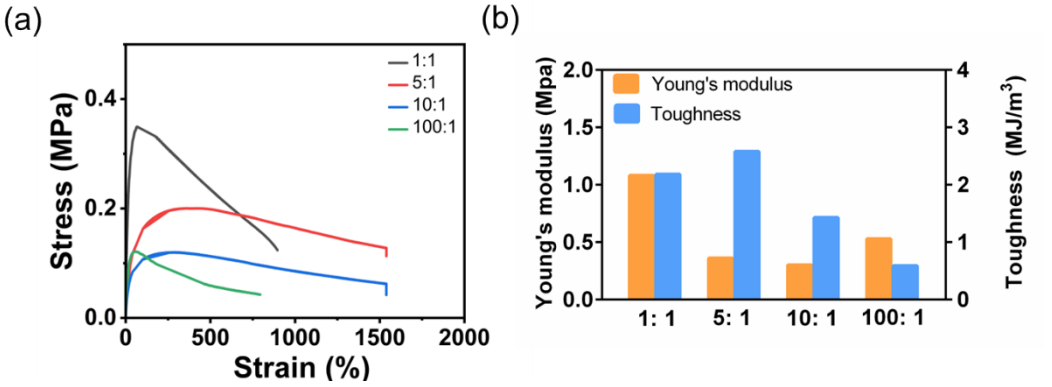

Figure S12. The elasticity of poly[**TA-MoS$_2$**]. (a) The strain-stress curves of poly[**TA-MoS$_2$**]; (b) the Young's moduli and toughness of poly[**TA-MoS$_2$**].

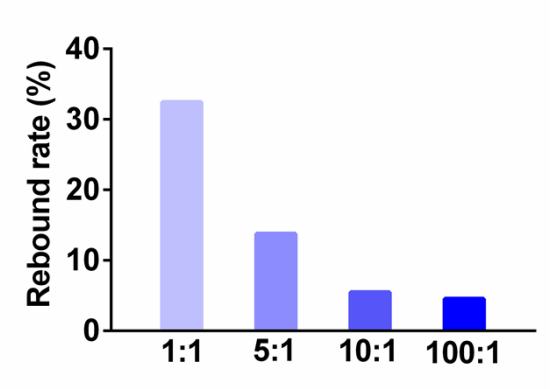

Figure S13. The rebound rates of poly[**TA-MoS$_2$**].

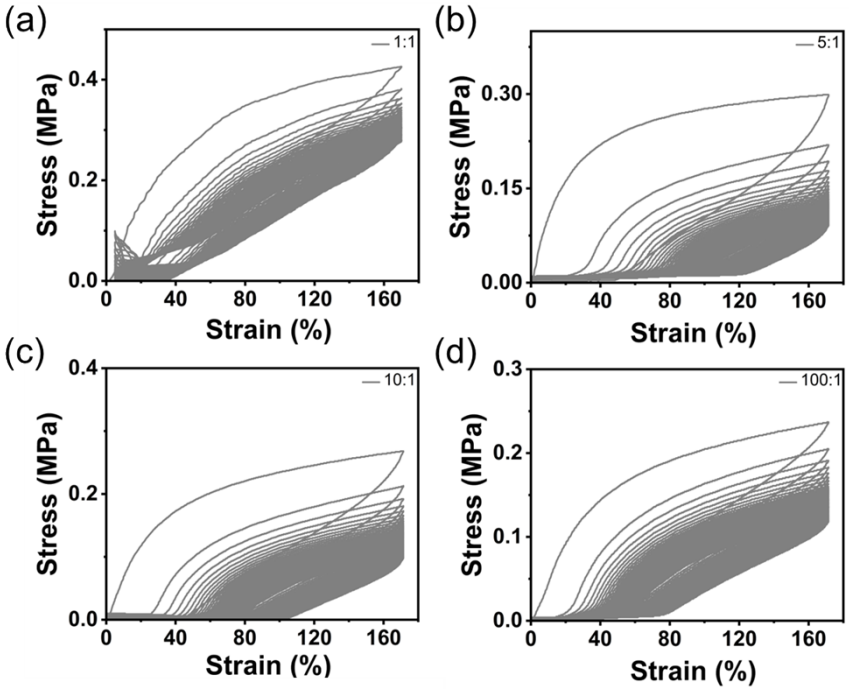

Figure S14. Cyclic loading-unloading curves of poly[**TA-MoS$_2$**]. (a) 1: 1; (b) 5: 1; (c) 10: 1; and (d) 100: 1.

15. Adhesion properties

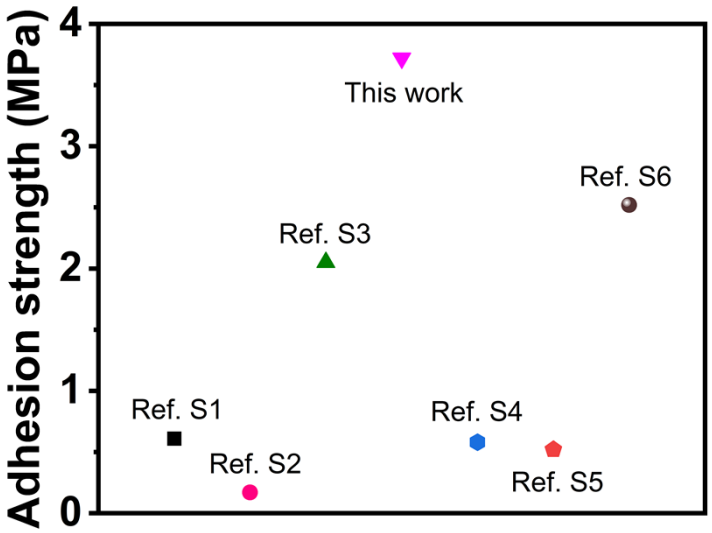

Figure S15. Comparison of supramolecular adhesives used in this study and reported **TA**-based adhesives toward glass.

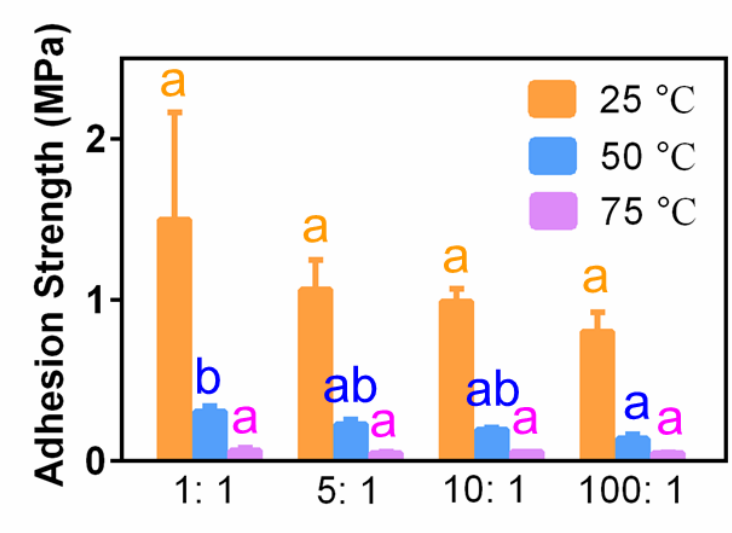

Figure 16. The adhesion strengths of poly[**TA-MoS_2**] under different temperature. Different letters signify significant differences at $p < 0.05$.

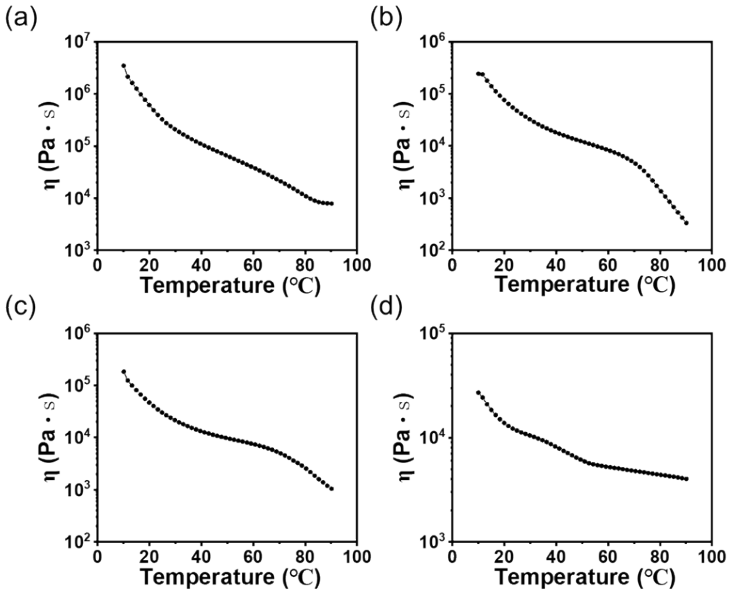

Figure 17. Viscosity (η) of poly[**TA-MoS$_2$**] at reversible temperature-dependent rheological tests. (a) 1: 1; (b) 5: 1; (c) 10: 1; and (d) 100: 1.

16. 3D printing of poly[TA-MoS$_2$]

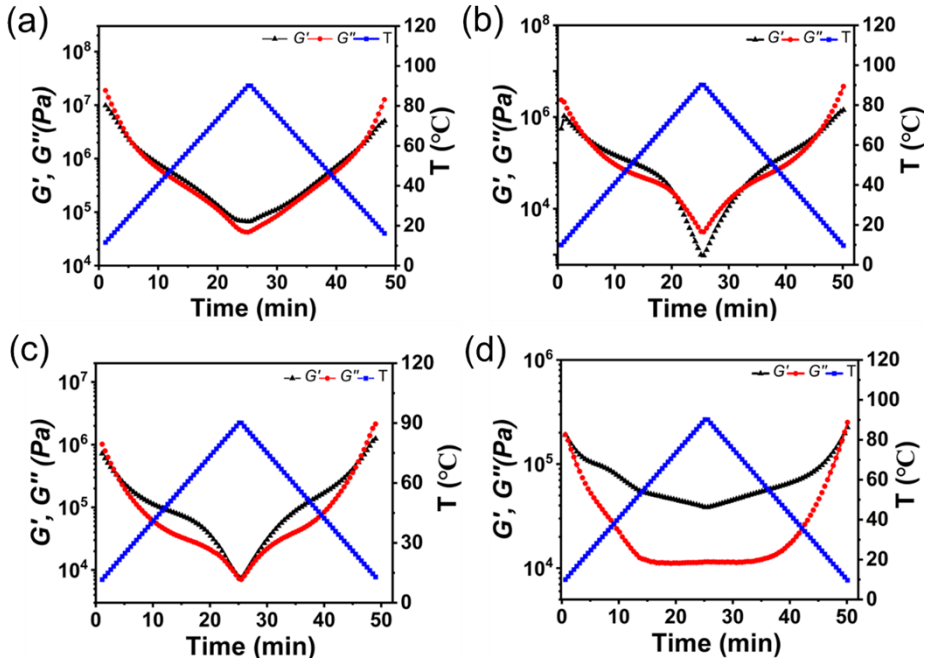

Figure S18. *G'* and *G''* values of poly[**TA-MoS$_2$**] at reversible temperature-dependent rheological tests: (a) **TA**: **MoS$_2$** = 1: 1; (b) **TA**: **MoS$_2$** = 5: 1; (c) **TA**: **MoS$_2$** = 10: 1; (d) **TA**: **MoS$_2$** = 100: 1.

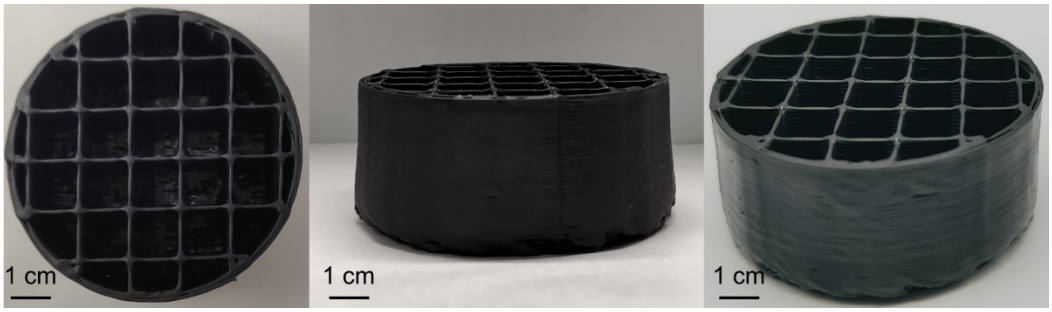

Figure S19. 3D-printed models of poly[**TA-MoS_2**] (**TA**: **MoS_2** = 10: 1).

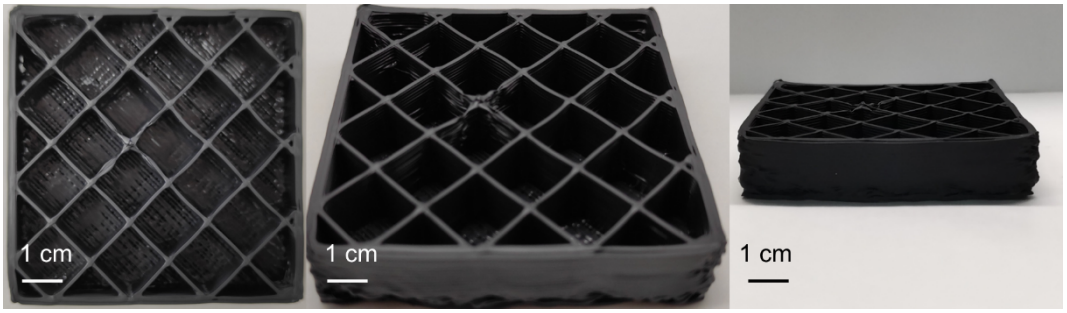

Figure S20. 3D-printed models of poly[**TA-MoS_2**] (**TA**: **MoS_2** = 10: 1).

17. References

[S1] G. Yao, F. Li, and S. Dong, *Chem. Eng. Sci.*, 2023, **281**, 119164.

[S2] J. Chen, D. Guo, S. Liang, and Z. Liu, *Polym. Chem.*, 2020, **11**, 6670–6680.

[S3] Z. Chen, C. Song, X. Lian, B. Xu, and Y. Wang, *Adv. Funct. Mater.*, 2024, DOI: 10.1002/adfm.202400829.

[S4] J. Li, Y. Zhang, Q. Zhang, C. Cai, F. Li, and S. Dong, *Adv. Mater. Interfaces*, 2023, **10**, 2202005.

[S5] B. Sieredzinska, Q. Zhang, K. J. van den Berg, J. Flapper and B. L. Feringa, *Chem. Commun.*, 2021, **57**, 9838–9841.

[S6] Q. Zhang, C.-Y. Shi, D.-H. Qu, Y.-T. Long, B. L. Feringa, and H. Tian, *Sci. Adv.*, 2018, **4**, eaat8192.